A Lymph Node Targeted Adjuvant and Engineered Subunit Vaccine Promotes Potent Immunity to Epstein-Barr Virus in HLA-expressing Mice

Vijayendra Dasari
Queensland Institute of Medical Research https://orcid.org/0000-0003-2106-0945
Lisa McNeil
Elicio Therapeutics
Kirrilee Beckett
QIMR Berghofer Medical Research Institute
Matthew Solomon
QIMR Berghofer Medical Research Institute
George Ambalathingal
QIMR Berghofer Medical Research Institute
Martin Steinbuck
Elicio Therapeutics
Aniela Jakubowski
Elicio Therapeutics
Lochana Seenappa
Elicio Therapeutics
Erica Palmer
Elicio Therapeutics
Jeff Zhang
Elicio Therapeutics
Chris Haqq
Elicio Therapeutics https://orcid.org/0000-0001-8600-9548
Peter DeMuth
Elicio Therapeutics
Rajiv Khanna (rajiv.khanna@qimr.edu.au)
QIMR Berghofer Medical Research Institute https://orcid.org/0000-0003-2241-0353

Article

Keywords:

Posted Date: July 13th, 2022

DOI: https://doi.org/10.21203/rs.3.rs-1763329/v1

Version of Record: A version of this preprint was published at Nature Communications on August 8th, 2023. See the published version at https://doi.org/10.1038/s41467-023-39770-1.

Abstract

Recent emergence of a causal like between Epstein-Barr virus (EBV) and multiple sclerosis has generated considerable interest in the development of an effective vaccine against EBV. Here we describe a novel vaccine formulation based on a lymph node targeting Amphiphile (AMP) vaccine adjuvant, AMP-CpG, admixed with EBV gp350 glycoprotein and a novel EBV-polyepitope protein (EBVpoly) that includes 20 $CD8^+$ T-cell epitopes from EBV latent and lytic antigens. Potent gp350-specific IgG responses were induced in mice with titers > 100,000 in AMP-CpG vaccinated mice. Immunization including AMP-CpG also induced high frequencies of polyfunctional gp350-specific $CD4^+$ T-cells and EBVpoly-specific $CD8^+$ T-cells that were 2-fold greater than soluble CpG and were maintained for > 7 months post immunization. This combination of broad humoral and cellular immunity against multiple viral determinants is likely to provide better protection against primary infection and control of latently infected B cells leading to protection against the development of EBV-associated diseases.

Teaser: A lymph node targeted AMP-CpG subunit EBV vaccine induces potent and durable immunity in HLA expressing mice.

Introduction

Epstein-Barr virus (EBV) is a gamma herpesvirus and is a ubiquitous human pathogen, infecting at least 95% of the world's adult population. During primary infection EBV is generally transmitted through saliva and infects resting B cells or epithelial cells in the oropharynx and then triggers transcriptional programming of B cells to establish life-long viral latency [1]. Although, primary EBV infection in children is asymptomatic or mildly symptomatic, acquisition of EBV infection in adolescents or young adults causes symptomatic infectious mononucleosis (IM)[2]. In addition to significant primary infection-associated morbidity, IM is considered to be a major risk factor for the future development of multiple EBV-associated diseases including multiple sclerosis (MS) and Hodgkins lymphoma [3,4]. In addition, EBV is also considered the primary etiological agent associated with multiple lymphoid and epithelial cancers with about 200,000 new EBV-associated cancers diagnosed worldwide each year [5,6].

Several prophylactic and therapeutic approaches are in various stages of development, but no medical intervention for EBV infection has been licensed to date [1,7]. In EBV infected individuals, serum antibodies directed against EBV-encoded glycoproteins (e.g. glycoprotein 350, gp350) are able to neutralize EBV to prevent infection of B cells and epithelial cells [8–11]. Human phase II clinical trials with gp350/AS04 vaccination demonstrated clinical efficacy in preventing the development of acute IM but did not prevent EBV infection [12]. Although preexisting neutralizing antibodies provide a first line of defense against acute viral infection, it is now well established that effective long-term control of latently infected B cells is critically dependent on T cell-mediated immunity. Therefore, induction of potent and durable T cell immunity through vaccination may prevent establishment or progression of latent EBV infection and the subsequent development of etiologically related autoimmune diseases and cancers.

Based on these observations, optimal EBV vaccines designed to control primary and latent infection will need to induce both humoral and cellular immune responses targeted to viral glycoproteins, lytic and latent antigens including EBV nuclear antigens and latent membrane proteins. Subunit vaccination is an attractive strategy for this purpose, however, full-length EBV latent proteins can trigger oncogenesis by blocking apoptosis, promoting genomic instability and supporting uncontrolled cell proliferation which limits their use as vaccine immunogens [13,14]. Moreover, polyvalent strategies requiring manufacturing and coformulation of numerous protein immunogens required to induce the necessary breadth of immunity may not be feasible due to challenging cost and complexity of manufacturing. Accordingly, we have developed a novel strategy to specifically target multiple latent and lytic EBV protein epitopes which overcomes these factors limiting their use in a vaccine formulation. Extensive mapping of human $CD8^+$ T cell epitopes from EBV antigens has allowed us to design a polyepitope vaccine immunogen (EBVpoly) which incorporates multiple $CD8^+$ T cell epitopes into an engineered protein immunogen. Here, individual HLA-restricted antigenic peptide sequences identified from a variety of EBV antigens are included in series and separated by proteolytic cleavage sites creating a structure resembling “beads on a string” [15–18]. Preclinical studies have shown that this polyepitope vaccine strategy is highly effective in inducing anti-viral T cell immunity targeting EBV and CMV [16,17,19]. Coformulation of EBVpoly with whole recombinant gp350 protein presents an opportunity to generate EBV-neutralizing humoral responses in concert with cellular immunity to enhance prophylactic activity alongside persistent control of EBV latency.

In addition to immunogen selection, incorporation of immunomodulatory adjuvants in vaccine design can determine the strength and character of the resulting immune response. Molecular adjuvants, including TLR agonists, are attractive options for use in subunit vaccines given their potential for simple co-formulation and potent immunomodulation in support of adaptive immunity. However, rapid capillary absorption of low molecular weight adjuvants (< 20 kDa) at the injection site leads to limited accumulation in draining lymph nodes where adaptive immune responses are orchestrated. In contrast, larger macromolecules and proteins, including many subunit immunogens, are restricted from transit across the vascular endothelium by multiple size-dependent anatomical structures, leading to preferential drainage from tissue through afferent lymphatics. To address this challenge, we have utilized an Amphiphile (AMP)-modified CpG DNA adjuvant (AMP-CpG) designed to enhance lymph node delivery and accumulation. Here, diacyl-lipid conjugation to TLR-9 stimulatory CpG DNA facilitates association with endogenous tissue albumin (~ 65 kDa) at the injection site to achieve specific targeting to the draining lymph nodes where early activation of immune response is initiated [20–24]. Co-administration with protein subunit immunogens of relatively large molecular size therefore allows for concerted accumulation of antigen and adjuvant in draining lymph nodes to promote potent immunity.

Using EBV gp350 and EBVpoly in combination with AMP-CpG, we have designed a vaccine formulation to stimulate potent and durable humoral and cellular immunity and assessed its immunogenicity in multiple HLA-expressing mouse models. The data show that this strategy elicits robust and persistent EBV-specific neutralizing antibodies and polyfunctional antigen-specific $CD4^+$ and $CD8^+$ T cell responses.

Results

- EBV vaccine design

To design a vaccine for EBV capable of inducing both humoral and T cell responses against multiple viral antigens, we employed a novel immunogen design strategy together with an optimal lymph node targeted adjuvant approach to ensure concerted delivery of T and B-cell epitopes with lymphatic immune activation. We first designed EBV polyepitope protein, EBVpoly, a novel recombinant polyprotein with 20 $CD8^+$ T cell epitopes from eight different lytic and latent EBV antigens, linked together to form a “beads on a string” structure (Fig. 1A and 1B). The EBV epitopes were selected to target broad HLA coverage and multiple antigens representative of all phases of the EBV lifecycle. The HLA Class-I restricted A and B coverage of EBVpoly is 92% for the world population, with 94% coverage in the United States [25]. To facilitate effective epitope processing for HLA-presentation, the carboxy terminus of each epitope was joined by a proteasome liberation amino acid sequence (AD or K or R). These proteasomal liberation sequences were designed to improve the immunogenicity of the EBV $CD8^+$ T cell epitopes by facilitating proteasomal processing of the polyepitope protein after uptake by antigen presenting cells (APCs). EBVpoly protein was expressed using an *E. coli* BL21-codonPlus (DE3) RP protein expression host and was purified using Q Sepharose FF and phenyl sepharose columns (**Fig. S1**). The EBV gp350 protein was also included in the vaccine formulation as a known target for virus neutralization as well as $CD8^+$ and $CD4^+$ T cell responses. To promote robust lymphatic immune activation in concert with immunogen delivery, a lymph node-targeted AMP adjuvant, AMP-CpG, was included (Fig. 1C). After peripheral administration, AMP-CpG (consisting of a diacyl lipid conjugated to TLR-9 agonistic CpG DNA) non-covalently associates with endogenous tissue albumin which is efficiently transported via afferent lymphatics to accumulate in draining lymph nodes [22]. While prior studies have shown the small molecular size of CpG DNA necessitates AMP-modification to achieve lymph node targeting, the larger size of EBVpoly and gp350 proteins predicts their effective transit from subcutaneous tissue into lymph [26]. Once in the lymph nodes, the vaccine components are designed to accumulate in APCs where AMP-CpG can stimulate immune activation [22,27] while EBVpoly is processed to yield distinct epitopes for MHC Class I presentation and gp350 is available for T and B cell recognition (Fig. 1D).

EBVpoly effectively stimulates effector responses in human T cells

To confirm that EBVpoly can be processed by APCs and presented on HLA Class I molecules to activate EBV-specific $CD8^+$ T cell responses in humans, peripheral blood mononuclear cells (PBMCs) from six healthy EBV seropositive donors, HLA-matched for the epitopes expressed in EBVpoly, were pre-incubated with EBVpoly and then cultured with IL-2 for 14 days. The expansion of the EBV-specific T cells was then assessed by intracellular cytokine staining (ICS) assay. EBVpoly induced simultaneous expansion of functional EBV-specific $CD8^+$ T cells to multiple EBV epitopes in all six donors evaluated (Fig. 2A). These expanded T cells showed polyfunctional effector function following stimulation with EBV peptide

epitopes as indicated by the expression of both IFNγ and TNFα (Fig. 2B). These data confirm that EBVpoly can be efficiently processed by APCs, yielding epitopes effectively presented on MHC and recognized by cognate human $CD8^+$ T cells to promote activation and effector function.

AMP-CpG is associated with improved accumulation of EBVpoly alongside persistent inflammation of local and distal lymph nodes

Transit of molecules to the lymph nodes from a peripheral injection site is known to correlate with molecular size [22,23] and the efficiency of lymphatic drainage can be further modulated in response to local adjuvant-mediated inflammatory activity [28]. To investigate the efficiency of lymph node accumulation of EBVpoly and gp350, we administered fluorescently labeled proteins in mice together with soluble CpG or AMP-CpG and analyzed tissue-associated fluorescent signal in whole lymph nodes by IVIS imaging. EBVpoly (~ 25 kDa) accumulation in local and distal lymph nodes was significantly enhanced by co-administration with AMP-CpG relative to soluble CpG 24 and 48 hours after injection (Fig. 3A-D**).** In soluble CpG immunized animals, EBVpoly was only detectable ~ 1.5-fold above mock injected control levels in inguinal lymph nodes 24 hours following administration. Co-administration with AMP-CpG induced persistent accumulation in both inguinal and axillary nodes as much as 9.8-fold above background at 24 and 48 hours suggesting a potential mechanism for AMP-CpG mediated enhancement of lymph node drainage and/or retention for small protein immunogens. In contrast, gp350 (~ 350 kDa) was observed in both local inguinal and distal axillary lymph nodes at 24 and 48 hours with similar levels of accumulation after soluble and AMP-CpG adjuvanted vaccination (**Fig. S2**).

Parallel observation of proteomic signatures of inflammation in draining lymph nodes was conducted through multiplexed assessment of a panel of inflammatory or immunomodulatory proteins including (1) growth factors, (2) Th1-associated pro-inflammatory cytokines, (3) Th-2 and regulatory cytokines, (4) chemokines, and (5) inflammasome-associated cytokines. Analysis of the proteomic milieu in inguinal lymph nodes at 24 hours revealed a similar profile of upregulation in animals immunized with soluble or AMP-CpG, characterized by comprehensive elevation of nearly all analytes evaluated (Fig. 3E**)**. For AMP-CpG, this profile was largely consistent with that observed in distal axillary lymph nodes, while soluble CpG did not induce significant upregulation of a majority of analytes in distal axillary lymph nodes. Inflammatory proteomic responses induced by soluble CpG largely reverted to baseline in inguinal lymph nodes at 48 hours, consistent with a complete attenuation of response in distal axillary lymph nodes at this time point (Fig. 3F). However, AMP-CpG-induced inflammatory protein signatures were largely maintained in local and distal lymph nodes at 48 hours suggesting a more durable and comprehensive induction of acute inflammation associated with improved lymph node targeting by AMP-mediated delivery.

- Cellular immune response

To evaluate the strength and character of EBV-specific T cells and further establish the effect of a lymph node-targeted adjuvant on EBV-specific cellular immunity, we compared vaccination with AMP-CpG to

soluble CpG in HLA transgenic mice. HLA-B*35:01 mice were primed and then boosted twice, each three weeks apart with gp350 and EBVpoly admixed with dose matched AMP-CpG or soluble CpG. EBV-antigen-specific cytokine-producing T cells in splenocytes were evaluated directly *ex vivo* at Week 7, one week post second boost. Adjuvant only control immunized mice did not induce detectable T cell responses, while mice immunized with AMP-CpG had significantly higher EBVpoly-specific $CD8^+$ $cytokine^+$ T cells compared to mice dosed with soluble CpG (Fig. 4A-C). Approximately 11% of $CD8^+$ T cells produced either IFNγ, TNFα, IL-2 or both IFNγ and TNFα in AMP-CpG immunized mice, with 78% exhibiting polyfunctional secretion of two and/or three cytokines. By comparison, immunization with soluble CpG induced only 5% $CD8^+$ T cell responses. $CD8^+$ T cell responses after AMP-CpG immunization were also observed for other HLA transgenic mice, A*24:02 and B*08:01 at higher levels than soluble CpG, although frequencies of cytokine positive cells were lower than observed in B*35:01 mice (Fig. 4D). Cytokine-producing $CD4^+$ T cells in splenocytes stimulated *ex vivo* with gp350 overlapping peptides (OLPs) were also evaluated. AMP-CpG induced robust gp350-specific $CD4^+$ $cytokine^+$ T cells, ~ 3-fold higher than observed in soluble CpG immunized comparator mice (Fig. 4E and 4F) with correlated improvements in polyfunctional cytokine secretion (59% compared to 33%, respectively, Fig. 4G). EBV gp350-specific $CD4^+$ T cell responses were also induced in the other HLA transgenic mice, albeit at lower frequencies (Fig. 4H). AMP-CpG immunization also induced three-fold higher gp350-specific $CD8^+$ T cells than observed in adjuvant-only control treated animals with approximately 1.7% $cytokine^+$ cells at Week 7 (**Fig. S3**). Further, $CD4^+$ and $CD8^+$ T cell responses to both EBVpoly and gp350 were observed in draining inguinal and axillary lymph nodes (**Fig. S4**).

To enrich for EBV-specific memory T cells, splenocytes from the immunized mice were stimulated with EBVpoly $CD8^+$ T cell peptides or gp350 OLPs for 10 days, then assessed for the frequency of antigen-specific cytokine-producing T cells. Splenocytes from AMP-CpG immunized mice exhibited a dramatic expansion of EBVpoly-specific $cytokine^+$ $CD8^+$ T cells in B*35:01 mice compared to soluble CpG comparators, with 65% and 42% $cytokine^+$ cells, respectively (Fig. 5A and 5B). These $CD8^+$ T cells exhibited strong polyfunctional effector phenotype with most cells secreting two or three cytokines (Fig. 5C). High frequencies of $cytokine^+$ $CD8^+$ T cell responses were also observed in expanded splenocytes from AMP-CpG immunized A*02:01 HLA transgenic mice as compared to soluble CpG immunized mice (Fig. 5D). Similar trends were observed for $CD4^+$ T cells expanded and restimulated with gp350 OLPs, with an average of 17% and 11% $cytokine^+$ $CD4^+$ T cells in AMP-CpG and soluble CpG vaccinated mice, respectively (Fig. 5E-G). $Cytokine^+$ $CD4^+$ T cells were also increased after AMP-CpG immunization over adjuvant only controls for A*02:01 and B*08:01 HLA transgenic mice (Fig. 5H). Taken together, these data confirm the potent cellular immunogenicity of EBVpoly and further demonstrate the importance of effective adjuvant lymph-node targeting to optimally induce polyfunctional $CD8^+$ and $CD4^+$ T cells in mice.

Humoral immune response

Potent IgG responses including neutralizing activity are critical to providing effective protection against primary EBV infection of B cells. To evaluate gp350-specific B cell responses in B*35:01 transgenic mice, splenocytes were tested in a gp350-specific B cell ELISpot. Mice immunized with AMP-CpG or soluble CpG induced comparable numbers of gp350-specific antibody secreting B cells when directly assessed *ex vivo* (Fig. 6A). Corresponding memory B cell responses were subsequently assessed by first inducing B cells to differentiate into antibody secreting cells (ASCs) for 3 days before assaying for gp350-specific antibody-secreting cells by B cell ELISpot assay. Increased numbers of memory gp350-specific ASCs were induced after immunization with AMP-CpG as compared to soluble CpG (Fig. 6B) indicating enhanced memory response quality associated with AMP-CpG adjuvant administration. Three weeks after the initial immunization, both cohorts showed robust gp350-specific serum IgG responses. However, post-dose peak antibody responses at Week 4 and 7 were significantly elevated among the AMP-CpG immunized cohort compared to the soluble CpG comparators (Fig. 6C). These trends were similar when assessed in A*02:01 and A*24:02 mice but no significant differences were observed in B*08:01 expressing animals (**Fig. S5**). We also evaluated the induced Ig subclasses and found that B*35:01 transgenic mice immunized with AMP-CpG had similar IgM and IgG3 (Th1 Ig isotype) titers compared to mice immunized with soluble CpG, while IgA, IgG1 (Th2 Ig isotype) IgG2a and IgG2b (Th1 Ig isotypes) titers were elevated in AMP-CpG immunized groups (Fig. 6D). Assessment in A*02:01, A*24:02, and B*08:01 expressing mice showed similar patterns of isotype induction with enhanced or equivalent titers observed after AMP-CpG immunization relative to soluble CpG comparators (**Fig. S5**). Finally, neutralizing antibody activity was assessed through an EBV-induced human B cell proliferation assay. Sera from AMP-CpG immunized mice exhibited approximately 100-fold increased neutralizing titers compared to soluble CpG vaccinated mice three weeks after the prime dose (Week 3) and one week post the second booster dose (Week 7, Fig. 6E). Similar to the increases in cellular immune responses stimulated by AMP-CpG, these data further demonstrate the potential for enhanced adjuvant lymphatic targeting to promote potent humoral immunity including substantially increased neutralizing activity important for preventing nascent viral infection.

- Long-term maintenance of cellular and humoral immune responses

Given the need for durable cellular immune responses against EBV to control the spread of latently infected B cells, circulating T cell responses were assessed longitudinally after three doses of EBV vaccine admixed with AMP-CpG or AMP-CpG adjuvant alone in HLA-B*35:01 transgenic mice. At all post-immunization time-points, the EBVpoly-specific $CD8^+$ T cell response in peripheral blood was significantly elevated in EBV-vaccinated mice compared to control mice. The peak of the EBVpoly-specific $CD8^+$ $cytokine^+$ T cell response was at Week 7, one week after the second boost with subsequent gradual contraction of the response through Week 29. Importantly, responses were maintained for greater than 6 months post immunization at higher levels than the control group (Fig. 7A and 7B). The induced EBV-specific $CD8^+$ T cells remained highly polyfunctional at Week 29, with 72% of cells secreting 2 or 3 cytokines (**Fig. S6**). *In vitro* stimulation of splenocytes to assess expansion of memory responses resulted in greatly increased frequency of EBVpoly-specific $CD8^+$ T cells at the long term timepoints

(Fig. 7C, **Fig. S7**). Mice from each cohort were recalled with a subsequent immunization at Week 30 and the recall response was evaluated one week later, at Week 31. Recall immunization increased the frequency of cytokine$^+$ CD8$^+$ T cells > 4-fold over Week 29 from 4–16% *ex vivo*, levels similar to earlier peak responses (Fig. 7D) with similar trends observed after expansion *in vitro* (**Fig. S8**). Similar results were seen with gp350-specific CD4$^+$ T cells, although the peak of the response was earlier than for CD8$^+$ T cells, at Week 4 (Fig. 7E **and F**). These CD4$^+$ T cell responses were maintained through Week 29 above adjuvant-only controls. Consistent with memory responses for CD8$^+$ T cells, greatly increased frequencies of cytokine$^+$ CD4$^+$ T cells were observed following *in vitro* expansion with gp350 OLPs (Fig. 7G, **Fig. S7**). The recall immunization also boosted gp350-specific CD4$^+$ T cells five-fold over the pre-recall timepoint, from 1–5% cytokine$^+$ CD4$^+$ T cells *ex vivo* (Fig. 7H) while expanded responses were comparable to earlier peak levels (**Fig. S8**). When compared to mice immunized with soluble CpG, CD8$^+$ T cell responses were 2-fold higher for AMP-CpG immunized mice, whereas CD4$^+$ T cell responses were similar between the two cohorts (**Fig. S7**). These data indicate that immunization with AMP-CpG stimulates long-lived CD4$^+$ and CD8$^+$ T cell responses including robust memory T cells capable of rapid expansion and polyfunctional cytokine secretion in response to subsequent exposure to EBV immunogens.

Durable antibody responses are also important to prevent infection and control the expansion of latently infected B cells. We evaluated gp350-specific B cell and anti-gp350 antibody responses at long term timepoints. Splenic gp350-specific ASCs were maintained at significantly elevated levels through Week 29, 7 months after the initial immunization with AMP-CpG (Fig. 8A). A recall immunization at Week 30 increased ASC responses to Week 7 peak levels (Fig. 8B). Memory ASCs were also durably elevated through 6 months and a subsequent recall on Week 30 boosted them to peak levels (Fig. 8C and 8D). Anti-gp350 IgG titers were maintained well above control group levels through Week 29 while the recall response increased IgG titers to similar peak levels observed at Week 4 (Fig. 8E and 8F). Evaluation of Ig subtypes showed that IgM, IgG1, IgG2a and IgG2b were durable for 7 months, but IgG3 titers were transiently elevated before decline by Week 14 (Fig. 8G). EBV neutralization activity of serum collected throughout the study showed a peak at Week 7 consistent with the observed peak in ASC response (Fig. 8H). Assessment at Week 29 showed maintenance of neutralizing activity above adjuvant-only background levels, and these were increased to near-peak levels at Week 31, 7 days following recall. Thus, immunization with AMP-CpG rapidly generated robust neutralizing antibody responses which are maintained for at least 7 months and are quickly boosted after recall exposure to EBV immunogens.

Discussion

EBV is classified as a class I carcinogen due to its high oncogenic potential and association with several lymphoid and epithelial cancers [29]. More recently, a definitive link has been established between EBV infection and subsequent MS [3,30]. Hence, prophylactic and therapeutic vaccines against EBV would have a substantial public health and economic impact. In addition, the success of prophylactic vaccines against hepatitis B and oncogenic strains of human papillomavirus in prevention of cancers has

triggered interest in the possibility of primary prevention of the EBV-associated cancers through vaccination. However, despite considerable efforts no EBV vaccine has been licensed for human use [31,32].

Previous studies in healthy virus carriers and patients with EBV-associated diseases have provided critical insights on the natural immune response to EBV. In the infected host, EBV establishes a complex life cycle characterized by differentially expressed proteins. Expression of viral proteins in specific stages of the viral cycle and their associated molecular interactions with host cells plays an important role in the establishment of latent EBV-infection in B cells. Primary and latent EBV infection is controlled through a broad array of immune effector pathways which includes neutralizing antibodies, natural killer cells, $CD8^+$ cytotoxic T cells and $CD4^+$ helper T cells directed against multiple EBV antigens [33,34]. Individuals with defective humoral and/or cellular immunity can develop life-threatening complications leading to uncontrolled proliferation of EBV-infected cells. This is best exemplified by outgrowth of EBV-infected B cells in immunocompromised transplant recipients which can be reversed by adoptive transfer of EBV-specific T cells [35]. These observations and accumulating evidence from adoptive immunotherapy studies suggest that an ideal vaccine should prevent acute symptoms of primary EBV infection through the induction of robust humoral and cellular immunity including neutralizing antibodies and EBV-specific $CD4^+$ and $CD8^+$ T cell responses. More importantly, these immune responses should be sustained long-term to prevent development of EBV-associated malignancies and autoimmune diseases which emerge long after the primary infection.

To achieve this goal, we have designed a multi-antigen-specific protein subunit vaccine which includes EBV-encoded gp350 and EBVpoly recombinant proteins. EBV gp350 is a predominant protein element of the EBV viral capsid responsible for mediating viral entry to host cells through interaction with complement receptor 2 (CR2/CD21). Prior clinical studies have established the potential for vaccine-induced gp350-targeted neutralizing antibody responses to inhibit viral infection resulting in reduction of acute IM [12]. However, previous response levels were not effective at preventing EBV infection, suggesting that more potent neutralizing activity or concomitant action through vaccine-induced cellular immunity may be necessary to improve prophylactic efficacy [36]. Accordingly, EBVpoly is a novel engineered recombinant protein, precisely designed to encode 20 different immunodominant $CD8^+$ T cell epitopes derived from multiple EBV lytic and latent antigens. These epitopes are restricted through 16 different HLA class I alleles which covers > 92% of the world-wide population. *In vitro* stimulation of human PBMCs from healthy virus carriers with EBVpoly protein expanded polyfunctional $CD8^+$ T cells which were directed to multiple EBV antigens. Previous studies have shown EBV-specific $CD8^+$ T cells play a crucial role in controlling the outgrowth of EBV infected cells [37] and adoptive immunotherapy with these effector T cells can offer therapeutic benefit against EBV-associated malignancies and multiple sclerosis [38–41].

We evaluated the immunogenicity of gp350 and EBVpoly proteins in combination with a lymph node-targeted molecular adjuvant, AMP-CpG, a lipid-modified TLR-9 agonistic DNA oligonucleotide, which is efficiently delivered to professional APCs in the lymph nodes and induces robust immune responses against co-administered protein immunogens [22,42]. Previous studies have shown that the AMP lipid

domain can mediate non-covalent binding of AMP-CpG to endogenous albumin in peripheral tissue to enable albumin to serve as an efficient chaperone promoting improved biodistribution into draining lymph nodes [43]. Indeed, lymph node proteomic analysis showed that AMP-CpG administration induced robust activation of local innate immune responses. Notably, these were coincident with the timing of immunogen entry to lymph nodes suggesting the potential for AMP-adjuvant to promote concerted exposure of lymph node immune cells to activation stimulus with antigen. Soluble CpG adjuvant however failed to optimally promote lymph node antigen accumulation or development of a robust inflammatory milieu. These trends were most notable in relation to EBVpoly, which was minimally present in draining lymph nodes when administered with soluble CpG. These changes in antigen biodistribution are consistent with past studies observing adjuvant-driven mechanisms for improving lymph node accumulation of co-administered protein antigens; for example *(i)* local recruitment, antigen acquisition, and lymphatic transit of phagocytes, *(ii)* enhancement of afferent lymph flow, and *(iii)* optimization of antigen capture by lymph node resident innate immune cells have been previously reported [28,44,45]. These mechanisms may be promoted by AMP-CpG given the significant improvement in EBVpoly accumulation to draining lymph nodes associated with AMP-CpG relative to soluble CpG comparators. The lack of similar improvements with gp350 suggests the underlying mechanisms may be dependent on immunogen size or overall physical properties. Indeed, larger macromolecules are known to exhibit impaired convection through extracellular matrix, thus restricting access to the initial lymphatic vessels [46], a prerequisite for improved lymph node uptake mediated by adjuvant-driven enhancements to passive immunogen lymphatic transport and lymph node retention.

Consistent with enhancements to lymph node antigen trafficking and concerted upregulation of inflammatory proteomic signatures, EBV vaccine formulated with AMP-CpG induced robust EBV-specific cellular and humoral immune responses in multiple HLA transgenic mice and these responses were significantly higher when compared to soluble CpG adjuvanted comparators. Cellular immune responses were polyfunctional with a majority of T cells expressing two or more cytokines and included both $CD8^+$ and $CD4^+$ T cells directed to latent and lytic antigens and to gp350. Notably, previous studies have shown that EBV-specific $CD4^+$ T cells play an important role in prevention of early-phase EBV-induced B cell proliferation [47]. Antibody responses induced by the AMP-CpG formulated EBV vaccine showed 16-25-fold higher neutralizing titers when compared to vaccine formulation with soluble CpG. More importantly, neutralizing antibody titers in AMP-CpG vaccinated mice were 50-fold higher than those seen in healthy virus carriers [9,12,48,49]. Previous studies have shown that acquisition of EBV-specific neutralizing antibodies is coincident with the recovery from acute IM [48,50], suggesting the potential for immunization with AMP-CpG to promote enhanced immune control of primary infection and prevention of progression to symptomatic IM.

Another important aspect of EBV vaccine development is the long-term persistence of immune responses which are not only crucial for durable prevention of primary infection but may also play an important role in blocking the development of EBV-associated malignancies and autoimmune disorders. Both cellular and humoral immune responses induced by AMP-CpG formulated EBV vaccine were sustained for over 7

months in mice. Interestingly, the anti-gp350 IgG titers largely remained unchanged during the follow up period, consistent with durable elevation of serum neutralizing activity. While there was a drop in the *ex vivo* frequency of antigen-specific $CD8^+$ and $CD4^+$ T cells, *ex vivo* restimulation with HLA matched peptide epitope rapidly expanded these T cells, with a majority showing a polyfunctional profile. This was consistent with the rapid expansion of T cell responses *in vivo* following recall immunization of vaccinated mice which restored response frequencies to peak levels confirming the presence of durable functional memory responses following vaccination with AMP-CpG. Long-term persistence of cellular and humoral immunity may provide more robust protection against EBV-associated diseases. It is also important to emphasize that while vaccine formulations based on EBV glycoproteins (gp350, gH/gL and gH/gL/gp42) have shown some protection against EBV infection in humanized mice [51], it is unlikely that the antibodies directed to these glycoproteins alone can offer protection against latent EBV infection. In contrast, previous studies have clearly demonstrated that adoptive immunotherapy with latent antigen-specific T cells can reverse the outgrowth of EBV malignancies and offer clinical benefit to patients with progressive MS [41,52–54]. Therefore, vaccine-induction of cellular immunity alongside neutralizing antibody responses with broad specificity against targets spanning the viral lifecycle offers an attractive opportunity to improve prevention of disease associated with primary infection (IM) and chronic latent infection (MS and EBV-driven malignancy).

Collectively, data presented here clearly demonstrate that EBV protein subunit vaccine formulated with AMP-CpG can generate robust virus-specific cellular and humoral immunity which is persistent and capable of rapid expansion upon recall through exposure to EBV antigens. These studies provide an important platform for future clinical assessment of this vaccine formulation in human volunteers.

Materials And Methods

EBV polyepitope design, protein expression and purification

Twenty different $CD8^+$ T cell epitopes derived from lytic and latent EBV antigens were selected (Fig. 1B). The carboxyl terminus of each epitope was joined by a proteasome liberation amino acid sequence (AD or K or R). Proteasome liberation amino acid sequences improve the immunogenicity of $CD8^+$ T cell epitopes by enhancing proteasomal processing of the polyepitope protein by APCs [55]. To achieve high level of EBVpoly protein expression, the amino acid sequence of the EBVpoly construct was translated into DNA sequence using optimized *E. coli* codons and the protein-encoding DNA sequence was synthetically constructed and cloned into an isopropyl–β-D-thiogalactopyraniside (IPTG) inducible plasmid, pJexpress 404 (Atum Bio, CA, United States). Chemically competent BL21-codonPlus (DE3) RP *E. coli* cells (Agilent Technologies, CA, United States) were transformed with the inducible EBVpoly expression plasmid. To initiate protein expression culture was scaled up to 3L (Terrific Broth containing ampicillin) and then EBVpoly protein expression was induced by adding 1 mM IPTG per mL of culture and incubating for 6 hours at 25°C. At the end of the induction phase, the culture was harvested, and cells were lysed. Due to the high hydrophobic nature of the linear $CD8^+$ T cell epitopes, the induced EBVpoly

protein was aggregated in the form of inclusion bodies (IBs). Inclusion bodies were further purified by washing them with TE buffer (25 mM Tris and 5 mM EDTA) and EBVpoly protein solubilized in 50 mM NaH_2PO4, 10 mM Tris, 5 mM DTT, 8M urea, pH 9.5 buffer. The pH of the solubilized protein was then decreased to pH 7.0. To eliminate the host DNA and lipid contaminants solubilized protein was passed through the Q Sepharose FF column (Cytiva Sweden AB, Uppsala Sweden) and then EBVpoly was purified using phenyl sepharose column (Cytiva Sweden AB, Uppsala Sweden).

gp350 expression and purification

EBV gp350 nucleotide sequence encoding the extracellular domain was cloned in to a mammalian expression system and splice site mutations were carried out as outline previously [49]. The gp350 encoding vector was then transfected into CHO cells. Transfected CHO cell culture was scaled up and gp350 protein was purified from cell culture supernatant using cation, anion exchange and size exclusion chromatography techniques in a sequential manner [56]. Final purified gp350 was stored in 20 mM histidine and 6% trehalose pH 6.0 buffer and purified protein was characterized using SDS-PAGE and Western blot analysis.

Animals and study design

Ethics approval to conduct animal experiments were obtained from QIMR Berghofer Medical Research Institute Animal Ethics committee under project number P2241. All human HLA expressing mice (HLA A1, HLA A2, HLA A24, HLA B8 and HLA B35) were obtained from Institut Pasteur (Paris, France). Mice were bred and maintained under pathogen-free environment at the QIMR Berghofer animal facility. Multiple HLA transgenic mice (HLA B35, B8, A2 or A24) that are deficient in expressing mouse MHC class I molecule and contain transgenes of the commonly expressed human HLA class I molecules were used [57]. Two groups of 6 – 8 weeks old female mice (n = 6) for each HLA transgene were immunized with 3 doses of EBV vaccine comprising 40 µg of EBVpoly and 10 µg of gp350 proteins, formulated with either 1.2 nmol AMP-CpG-7909 (Elicio Therapeutics, *Boston, Massachusetts, United States*) or 1.2 nmol CpG-7909 (InvivoGen, *San Diego, CA, United States*). Another two groups of mice (n = 4) were injected with 3 doses of 1.2 nmol AMP-CpG-7909 or 1.2 nmol CpG-7909 to serve as placebo (adjuvant-alone control) group. All injections were administered subcutaneously, 50 µl at each side of the tail base (100 µl total) on day 0, weeks 3 and 6. The mice were tail bled on week 3, 4 and 6, and were finally sacrificed at Week 7. For long-term immunogenicity evaluation, multiple groups of HLA B35 mice were immunized with vaccine (n = 36) or control (n = 24) formulations as mentioned above. Mice were sacrificed on weeks 4, 7, 21 and 29. To determine the recall response, mice (n = 9) were immunized with a booster dose on week 30 and these mice were sacrificed after 7 days, at week 31. Blood, spleen, inguinal and axillary

lymph nodes were collected to assess EBV-specific humoral and cell-mediated responses using ICS assays, gp350 ELISpot, ELISA, and neutralizing antibody assays.

Biodistribution and lymph node activation assays:

AlexaFluor (AF) 594-maleimide fluorophore (Thermo Fisher Scientific, Cat No. A10256) was thioether-coupled to EBVpoly protein at pH 7.0-7.5 in the presence of reducing agent TCEP [tris(2-carboxyethyl)phosphine]. The reaction was allowed to proceed at RT for 2 hours and protein precipitates were formed. After centrifugation, the protein pellet was resuspended in 6M guanidine hydrochloride solution at 2 mg/ml. In contrast, cysteine residues of EBV gp350 protein are not accessible even after TCEP treatment. Therefore, thiol groups were introduced onto the gp350 protein. SPDP-Peg4-NHS (Quanta Biodesign, Cat No. 10374) was added to the gp350 PBS solution and incubated at RT for 30 min. gp350-SPDP was treated with TCEP and AF647-maleimide (Thermo Fisher Scientific, Cat No. A20347) for 2 hours at RT. gp350-AF647 was purified on PD-10 columns and subsequently concentrated on a lyophilizer and resuspended in PBS at 2 mg/ml. Animal studies were carried out under an institute-approved Institutional Animal Care and Use Committee (IACUC) protocol following federal, state, and local guidelines for the care and use of animals. C57Bl/6J mice were immunized with 8 µg EBVpoly-AF594 and 10 µg gp350-AF647 admixed with 1.2 nmol soluble- or AMP-CpG. Fluorescent negative controls received equivalent amounts of AMP-CpG and unlabeled antigen. Mock-treated animals were administered vehicle alone (25mM glycine, pH 4.5). Lymph nodes were harvested from immunized animals 24 and 48 hours post vaccine administration and imaged *ex vivo* using the In Vivo Imaging System (IVIS) Spectrum CT. AF594 fluorophore was excited at 570 nm and detected at 620 nm, and AF647 fluorophore was excited at 640 nm and detected at 680 nm. Lymph nodes were further processed for proteomic analysis by Luminex to determine their cytokine/chemokine content. Protein Extraction Buffer (Invitrogen, cat# EPX-9999-000) contained Mini protease inhibitor cocktail (Roche, cat # 53945000) and HALT phosphatase inhibitors (diluted 1:100, Thermo Fisher Sci cat# 78442). Lymph nodes were homogenized using a TissueLyser II (Qiagen). Cleared lysates were analyzed with Luminex Cytokine and Chemokine kits (EMDMillipore, cat# MCYTOMAG-70K and #MECY2MAG-73K) according to the manufacturer's instructions.

Evaluation of EBVpoly immunogenicity in human PBMCs

The study was approved by QIMR Berghofer Medical Research Institute Human Research Ethics Committee under project number P2282 and all healthy volunteers who offered blood samples gave written informed consent. PBMC from six different HLA-mapped, EBV-seropositive, healthy donors were stimulated with 25 µg of EBVpoly protein for 1 hour at 37°C. Then, cells were washed with RPMI supplemented with 10% FCS and cultured for 14 days to allow for T cell expansion; cultures were supplemented with medium containing RPMI and human recombinant IL-2 on days 2, 5, 8 and 11.

Following *in vitro* expansion of EBV-specific $CD8^+$ T cells from healthy seropositive donors, cells were washed and then stimulated with 0.2 µg/mL of HLA matching peptides in the presence of human CD107a antibody conjugated to FITC (BD Pharmingen cat# 555800), Golgiplug™ and Golgistop™ (BD Biosciences; CA, United States) for 5 hours at 37°C and 6.5% CO_2. Cells were washed twice, then incubated with Live/Dead™ near IR (Invitrogen, cat# L34976), Pacific Blue™-conjugated anti-CD4 (BD Pharmingen, cat# 558116) and PerCPCy5.5-conjugated anti-CD8 (eBioscience, cat# 45008842)). Cells were fixed and permeabilized using a BD Cytofix/Cytoperm™ kit (BD Biosciences; CA, United States). Then cells were incubated with PE-conjugated anti IL-2 (eBioscience, cat# 12702942), APC-conjugated anti TNFα (Biolegend, cat# 502912) and AF700-conjugated anti IFNγ (BD Biosciences cat# 557995) to determine intracellular cytokine secretion. Cells were acquired on a BD FACSCanto™ II and data was analyzed using FlowJo™ software (Becton, Dickinson and Company, OR, United States).

gp350 ELISA.

Serum total anti-gp350 antibody was evaluated by an enzyme-linked immunosorbent assay (ELISA). Briefly, immunosorbent 96-well plates were coated with 50 µL of recombinant EBV gp350 protein (2.5 µg/mL of gp350 protein diluted in phosphate buffer saline) and plates were incubated at 4°C overnight. Plates were washed with phosphate buffer saline containing 0.05% Tween 20 (PBST) and then blocked with 5% skim milk. Serially diluted serum samples were added and incubated for 2 hours at room temperature. After washing with PBST, plates were incubated with HRP-conjugated sheep anti-mouse Ig antibody (to determine total antibody response) (SouthernBiotech, cat# 1010-05) for 1 hour. These plates were washed and incubated with 3,3',5,5'-Tetramethylbenzidine (TMB) substrate solution (invitrogen, cat#00420156) for 10 minutes and then color development was stopped by adding 1N HCl. Optical density (OD) at 450 nm was measured using an ELISA Biotek Power Wave Plate reader. The OD_{450} nm value of 0.5 was considered as baseline value and above 0.5 was regarded as positive response. The maximum dilution to give a positive result was used as the endpoint antibody titer.

Antibody isotype analysis

Briefly, immunosorbent 96-well plates coated with recombinant gp350 were processed as described above and incubated with HRP-conjugated goat anti-mouse IgA (SouthernBiotech, cat# 1010-05), IgM (SouthernBiotech, cat# 1020-05), IgG1 (SouthernBiotech, cat# 1070-05), IgG2a (SouthernBiotech, cat# 1080-05), IgG2b (SouthernBiotech, cat# 1090-05) or IgG3 (SouthernBiotech, cat# 1100-05) antibody for 1 hour. Plates were subsequently washed and incubated with TMB substrate solution for 10 minutes followed by 1N HCl and analysis using an ELISA Biotek Power Plate reader and endpoint antibody titer was calculated as mentioned above.

EBV neutralization assay

Sera were pooled per timepoint to assess the ability to neutralize EBV using an EBV induced B cell proliferation assay. Briefly, the pooled serum samples were heat inactivated at 56° C for 30 minutes. The samples then were serially diluted in duplicates, in 2-fold dilutions (from 1:2 to 1:4096 dilution), in 25 µL volumes in a 96 well U-bottom well plate. The B95-8 EBV viral isolate was added to the diluted serum samples in a 25 µL volume (50 µL/well total). The serum/virus mixture was incubated for two hours at 37°C. PBMCs (100,000 cells in 50 µL/well) from EBV-seronegative donor labelled with CellTrace™ Violet (invitrogen, cat# C34557) were added and then incubated for one hour at 37°C and 6.5% CO_2. Cells were washed and incubated for 5 days at 37°C and 6.5% CO_2 to allow infection and proliferation of B cells from EBV seronegative donors. On day 5, cells were stained with Live/Dead™ near IR (invitrogen, cat# L34976), APC anti-human CD3 (BD Biosciences, cat# 340440), PE-cy5 anti-human CD19 (BD Pharmingen, cat# 555414). Cells were acquired on a BD FACSCanto™ II and data was analyzed using FlowJo™ software. The maximum dilution to reduce the number of proliferating B cells by more than 50% compared to the control (i.e., PBMC infected with B95-8 EBV with no serum) was used as neutralization titer.

B cell ELISpot

B cell ELISpot analysis was carried out using mouse IgG ELISpot kit (MAbtech AB, cat# 3825-2A). PVDF ELISpot plates were treated with 70% ethanol, washed five times with distilled water, coated with 100 µL/well EBV gp350 protein (25 µg/mL) or anti-IgG antibody (15 µg/mL) as a positive control and incubated overnight at 4°C. Plates were blocked with DMEM containing 10% serum and 3 x 10^5 cells/well, in triplicate from each mouse, was added and then incubated for 18 hours in a 37° C humidified incubator with 5% CO_2. Cells were removed and plates were washed. Detection antibody anti-IgG conjugated to HRP was added to each well and incubated for 2 hours at room temperature and then washed. Streptavidin-ALP was added to each well and incubated at room temperature for 1 hour, followed by washing and treating plates with substrate solution containing BCIP®/NBT (Sigma-Aldrich; MO, United States) until color development was prominent. Color development was stopped by washing plates with water and plates were kept for drying overnight before counting spots in an AID ELISpot reader.

To measure memory B cell response, splenocytes (5 x 10^5) from vaccine and control mice were activated with a mixture comprising the TLR7/8-agonist, R848 (resiquimod), and recombinant mouse IL-2 for three days in 24 well plate. Cells were washed three times and then counted. 2.5 x 10^4 cells were transferred to respective wells in triplicates. The ELISpot was carried out as described above. The number of spots was counted in an AID ELISpot reader and the number of positive spots was normalized to calculate ASCs per 3 x 10^5 splenocytes.

Ex vivo intracellular cytokine staining (ICS) assay.

Splenocytes were stimulated with either 0.2 µg/mL of HLA B35 (“HPV” and “LPEP”), HLA A2 (“GLC” and “CLG”), HLA A24 (“TYG” and “PYL”), HLA B8 (“FLR” and “RAK”) restricted peptides, or gp350 OLP PepMix™ EBV, a pool of 224 peptides derived from a peptide scan (15mers with 11 aa overlap) through envelope glycoprotein GP350/GP340 (Swiss-Prot ID: P03200) of Epstein-Barr virus (HHV4) (Product Code: PM-EBV-GP350/GP340; JPT Peptide Technologies GmbH, Berlin, Germany). Splenocytes were stimulated in the presence of Golgiplug™ and Golgistop™ for 5 hours in a 37° C humidified incubator with 6.5% CO_2. After incubation, cells were washed twice, then incubated with Live/Dead™ near IR (invitrogen, cat# L34976), FITC-conjugated anti-CD4 (BD Biosciences, cat# 553651) and PerCP5.5 conjugated anti-CD8 (BD Biosciences, cat# 551162). Cells were fixed and permeabilized using a BD Cytofix/Cytoperm™ kit, then incubated with PE-conjugated anti-IFNγ (BD Biosciences, cat# 554412), PE-Cy7 conjugated anti-TNFα (BD Biosciences, cat# 557844), and APC conjugated anti-IL-2 PE (BD Biosciences, cat# 554429). Cells were acquired on a BD FACSCanto™ II and data was analyzed using FlowJo™ software.

Expanded ICS assay.

Splenocytes (7 x 10^6) were stimulated with 1 µg/mL of HLA B35 (“HPV” and “LPEP”), HLA A2 (“GLC” and “CLG”), HLA A24 (“TYG” and “PYL”) and HLA B8 (“FLR” and “RAK”) restricted peptides or with 1 µg/mL of gp350 OLP PepMix™. Cells were cultured in a 24 well plate for 10 days at 37°C, 10% CO_2, and cultures were supplemented with IL-2 on days 2, 5 and 8. On day 10, the expanded T cells were stimulated with respective epitope peptides and then T cell specificity and polyfunctionality were assessed using multiparametric ICS assay, as described above.

References

1 Dasari, V., Bhatt, K. H., Smith, C. & Khanna, R. Designing an effective vaccine to prevent Epstein-Barr virus-associated diseases: challenges and opportunities. *Expert Rev Vaccines* **16**, 377-390, doi:10.1080/14760584.2017.1293529 (2017).

2 Balfour, H. H., Jr., Dunmire, S. K. & Hogquist, K. A. Infectious mononucleosis. *Clinical & translational immunology* **4**, e33, doi:10.1038/cti.2015.1 (2015).

3 Bjornevik, K. *et al.* Longitudinal analysis reveals high prevalence of Epstein-Barr virus associated with multiple sclerosis. *Science* **375**, 296-301, doi:10.1126/science.abj8222 (2022).

4 Handel, A. E. *et al.* An updated meta-analysis of risk of multiple sclerosis following infectious mononucleosis. *PLoS One* **5**, doi:10.1371/journal.pone.0012496 (2010).

5 Farrell, P. J. Epstein-Barr Virus and Cancer. *Annu Rev Pathol* **14**, 29-53, doi:10.1146/annurev-pathmechdis-012418-013023 (2019).

6 Taylor, G. S., Long, H. M., Brooks, J. M., Rickinson, A. B. & Hislop, A. D. The immunology of Epstein-Barr virus-induced disease. *Annual review of immunology* **33**, 787-821, doi:10.1146/annurev-immunol-032414-112326 (2015).

7 Dasari, V., Sinha, D., Neller, M. A., Smith, C. & Khanna, R. Prophylactic and therapeutic strategies for Epstein-Barr virus-associated diseases: emerging strategies for clinical development. *Expert Rev Vaccines* **18**, 457-474, doi:10.1080/14760584.2019.1605906 (2019).

8 Gu, S. Y. *et al.* First EBV vaccine trial in humans using recombinant vaccinia virus expressing the major membrane antigen. *Dev Biol Stand* **84**, 171-177 (1995).

9 Moutschen, M. *et al.* Phase I/II studies to evaluate safety and immunogenicity of a recombinant gp350 Epstein-Barr virus vaccine in healthy adults. *Vaccine* **25**, 4697-4705, doi:10.1016/j.vaccine.2007.04.008 (2007).

10 Bu, W. *et al.* Immunization with Components of the Viral Fusion Apparatus Elicits Antibodies That Neutralize Epstein-Barr Virus in B Cells and Epithelial Cells. *Immunity* **50**, 1305-1316 e1306, doi:10.1016/j.immuni.2019.03.010 (2019).

11 Ogembo, J. G. *et al.* A chimeric EBV gp350/220-based VLP replicates the virion B-cell attachment mechanism and elicits long-lasting neutralizing antibodies in mice. *J Transl Med* **13**, 50, doi:10.1186/s12967-015-0415-2 (2015).

12 Sokal, E. M. *et al.* Recombinant gp350 vaccine for infectious mononucleosis: a phase 2, randomized, double-blind, placebo-controlled trial to evaluate the safety, immunogenicity, and efficacy of an Epstein-Barr virus vaccine in healthy young adults. *J Infect Dis* **196**, 1749-1753, doi:10.1086/523813 (2007).

13 Morrison, J. A., Klingelhutz, A. J. & Raab-Traub, N. Epstein-Barr virus latent membrane protein 2A activates beta-catenin signaling in epithelial cells. *Journal of Virology* **77**, 12276-12284 (2003).

14 Lee, D. Y. & Sugden, B. The latent membrane protein 1 oncogene modifies B-cell physiology by regulating autophagy. *Oncogene* **27**, 2833-2842, doi:1210946 [pii]

10.1038/sj.onc.1210946 (2008).

15 Smith, C., Beagley, L. & Khanna, R. Acquisition of polyfunctionality by Epstein-Barr virus-specific CD8+ T cells correlates with increased resistance to galectin-1-mediated suppression. *J Virol* **83**, 6192-6198, doi:10.1128/JVI.00239-09 (2009).

16 Duraiswamy, J. *et al.* Induction of therapeutic T-cell responses to subdominant tumor-associated viral oncogene after immunization with replication-incompetent polyepitope adenovirus vaccine. *Cancer Research* **64**, 1483-1489 (2004).

17 Duraiswamy, J. *et al.* Therapeutic LMP1 polyepitope vaccine for EBV-associated Hodgkin disease and nasopharyngeal carcinoma. *Blood 2003.Apr.15.;101.(8.):3150.-6.* **101**, 3150-3156 (2003).

18 Thomson, S. A. *et al.* Minimal epitopes expressed in a recombinant polyepitope protein are processed and presented to CD8+ cytotoxic T cells: implications for vaccine design. *Proc.Natl.Acad.Sci.U.S.A.* **92**, 5845-5849 (1995).

19 Dasari, V. *et al.* Prophylactic and therapeutic adenoviral vector-based multivirus-specific T-cell immunotherapy for transplant patients. *Mol Ther Methods Clin Dev* **3**, 16058, doi:10.1038/mtm.2016.58 (2016).

20 Rakhra, K. *et al.* Exploiting albumin as a mucosal vaccine chaperone for robust generation of lung-resident memory T cells. *Sci Immunol* **6**, doi:10.1126/sciimmunol.abd8003 (2021).

21 Ma, L. *et al.* Enhanced CAR-T cell activity against solid tumors by vaccine boosting through the chimeric receptor. *Science* **365**, 162-168, doi:10.1126/science.aav8692 (2019).

22 Liu, H. *et al.* Structure-based programming of lymph-node targeting in molecular vaccines. *Nature* **507**, 519-522, doi:10.1038/nature12978 (2014).

23 Hanson, M. C. & Irvine, D. J. Synthesis of Lymph Node-Targeting Adjuvants. *Methods Mol Biol* **1494**, 145-152, doi:10.1007/978-1-4939-6445-1_10 (2017).

24 Appelbe, O. K. *et al.* Radiation-enhanced delivery of systemically administered amphiphilic-CpG oligodeoxynucleotide. *J Control Release* **266**, 248-255, doi:10.1016/j.jconrel.2017.09.043 (2017).

25 Bui, H. H. *et al.* Predicting population coverage of T-cell epitope-based diagnostics and vaccines. *BMC Bioinformatics* **7**, 153, doi:10.1186/1471-2105-7-153 (2006).

26 Trevaskis, N. L., Kaminskas, L. M. & Porter, C. J. From sewer to saviour - targeting the lymphatic system to promote drug exposure and activity. *Nat Rev Drug Discov* **14**, 781-803, doi:10.1038/nrd4608 (2015).

27 Seenappa, L. M. *et al.* Programming the lymph node immune response with Amphiphile-CpG induces potent cellular and humoral immunity following COVID-19 subunit vaccination in mice and non-human primates. *bioRxiv*, 2022.2005.2019.492649, doi:10.1101/2022.05.19.492649 (2022).

28 Silva, M. *et al.* A particulate saponin/TLR agonist vaccine adjuvant alters lymph flow and modulates adaptive immunity. *Sci Immunol* **6**, eabf1152, doi:10.1126/sciimmunol.abf1152 (2021).

29 Parkin, D. M. The global health burden of infection-associated cancers in the year 2002. *Int J Cancer* **118**, 3030-3044, doi:10.1002/ijc.21731 (2006).

30 Lanz, T. V. *et al.* Clonally expanded B cells in multiple sclerosis bind EBV EBNA1 and GlialCAM. *Nature*, doi:10.1038/s41586-022-04432-7 (2022).

31 Cohen, J. I., Fauci, A. S., Varmus, H. & Nabel, G. J. Epstein-Barr virus: an important vaccine target for cancer prevention. *Sci Transl Med* **3**, 107fs107, doi:10.1126/scitranslmed.3002878 (2011).

32 Taylor, G. S. & Steven, N. M. Therapeutic vaccination strategies to treat nasopharyngeal carcinoma. *Chin Clin Oncol* **5**, 23, doi:10.21037/cco.2016.03.20 (2016).

33 Munz, C. Redirecting T Cells against Epstein-Barr Virus Infection and Associated Oncogenesis. *Cells* **9**, doi:10.3390/cells9061400 (2020).

34 Jean-Pierre, V., Lupo, J., Buisson, M., Morand, P. & Germi, R. Main Targets of Interest for the Development of a Prophylactic or Therapeutic Epstein-Barr Virus Vaccine. *Front Microbiol* **12**, 701611, doi:10.3389/fmicb.2021.701611 (2021).

35 Khanna, R. *et al.* Activation and adoptive transfer of Epstein-Barr virus-specific cytotoxic T cells in solid organ transplant patients with posttransplant lymphoproliferative disease. *Proc.Natl.Acad.Sci.U.S.A.* **96**, 10391-10396 (1999).

36 Morgan, A. *et al.* Epstein-Barr virus vaccines. *Human herpesviruses: biology, therapy, and immunoprophylaxis.*, 1292-1305 (2007).

37 Khanna, R. & Burrows, S. R. Role of cytotoxic T lymphocytes in Epstein-Barr virus-associated diseases. *Annu.Rev.Microbiol.2000.;54.:19.-48.* **54:19-48.**, 19-48 (2000).

38 Rooney, C. M. *et al.* Use of gene-modified virus-specific T lymphocytes to control Epstein-Barr-virus-related lymphoproliferation. *Lancet* **345**, 9-13, doi:S0140-6736(95)91150-2 [pii] (1995).

39 Lin, C. L. *et al.* Immunization with Epstein-Barr Virus (EBV) peptide-pulsed dendritic cells induces functional CD8+ T-cell immunity and may lead to tumor regression in patients with EBV-positive nasopharyngeal carcinoma. *Cancer Res* **62**, 6952-6958 (2002).

40 Smith, C. *et al.* Pre-emptive and therapeutic adoptive immunotherapy for nasopharyngeal carcinoma: Phenotype and effector function of T cells impact on clinical response. *Oncoimmunology* **6**, e1273311, doi:10.1080/2162402X.2016.1273311 (2017).

41 Pender, M. P. *et al.* Epstein-Barr virus-specific T cell therapy for progressive multiple sclerosis. *JCI Insight* **3**, doi:10.1172/jci.insight.124714 (2018).

42 Steinbuck, M. P. *et al.* A lymph node-targeted Amphiphile vaccine induces potent cellular and humoral immunity to SARS-CoV-2. *Sci Adv* **7**, doi:10.1126/sciadv.abe5819 (2021).

43 Moynihan, K. D. *et al.* Enhancement of Peptide Vaccine Immunogenicity by Increasing Lymphatic Drainage and Boosting Serum Stability. *Cancer Immunol Res* **6**, 1025-1038, doi:10.1158/2326-6066.CIR-17-0607 (2018).

44 Gaya, M. *et al.* Host response. Inflammation-induced disruption of SCS macrophages impairs B cell responses to secondary infection. *Science* **347**, 667-672, doi:10.1126/science.aaa1300 (2015).

45 Lisk, C. *et al.* CD169+ Subcapsular Macrophage Role in Antigen Adjuvant Activity. *Front Immunol* **12**, 624197, doi:10.3389/fimmu.2021.624197 (2021).

46 Schudel, A., Francis, D. M. & Thomas, S. N. Material design for lymph node drug delivery. *Nat Rev Mater* **4**, 415-428, doi:10.1038/s41578-019-0110-7 (2019).

47 Nikiforow, S., Bottomly, K. & Miller, G. CD4+ T-cell effectors inhibit Epstein-Barr virus-induced B-cell proliferation. *J Virol* **75**, 3740-3752, doi:10.1128/JVI.75.8.3740-3752.2001 (2001).

48 Panikkar, A. *et al.* Impaired Epstein-Barr Virus-Specific Neutralizing Antibody Response during Acute Infectious Mononucleosis Is Coincident with Global B-Cell Dysfunction. *J Virol* **89**, 9137-9141, doi:10.1128/JVI.01293-15 (2015).

49 Jackman, W. T., Mann, K. A., Hoffmann, H. J. & Spaete, R. R. Expression of Epstein-Barr virus gp350 as a single chain glycoprotein for an EBV subunit vaccine. *Vaccine* **17**, 660-668 (1999).

50 Bu, W. *et al.* Kinetics of Epstein-Barr Virus (EBV) Neutralizing and Virus-Specific Antibodies after Primary Infection with EBV. *Clin Vaccine Immunol* **23**, 363-369, doi:10.1128/CVI.00674-15 (2016).

51 Wei, C. J. *et al.* A bivalent Epstein-Barr virus vaccine induces neutralizing antibodies that block infection and confer immunity in humanized mice. *Science translational medicine* **14**, eabf3685, doi:10.1126/scitranslmed.abf3685 (2022).

52 Bollard, C. M., Kuehnle, I., Leen, A., Rooney, C. M. & Heslop, H. E. Adoptive immunotherapy for posttransplantation viral infections. *Biol.Blood Marrow Transplant.* **10**, 143-155 (2004).

53 Gottschalk, S., Heslop, H. E. & Rooney, C. M. Adoptive immunotherapy for EBV-associated malignancies. *Leuk Lymphoma* **46**, 1-10, doi:X6NJBGGNJEVVJBYN [pii]

10.1080/10428190400002202 (2005).

54 Pender, M. P. *et al.* Epstein-Barr virus-specific adoptive immunotherapy for progressive multiple sclerosis. *Multiple sclerosis* **20**, 1541-1544, doi:10.1177/1352458514521888 (2014).

55 Dasari, V., Smith, C., Schuessler, A., Zhong, J. & Khanna, R. Induction of innate immune signatures following polyepitope protein-glycoprotein B-TLR4&9 agonist immunization generates multifunctional

CMV-specific cellular and humoral immunity. *Human vaccines & immunotherapeutics* **10**, 1064-1077 (2014).

56 Szakonyi, G. *et al.* Structure of the Epstein-Barr virus major envelope glycoprotein. *Nat Struct Mol Biol* **13**, 996-1001, doi:10.1038/nsmb1161 (2006).

57 Boucherma, R. *et al.* HLA-A*01:03, HLA-A*24:02, HLA-B*08:01, HLA-B*27:05, HLA-B*35:01, HLA-B*44:02, and HLA-C*07:01 monochain transgenic/H-2 class I null mice: novel versatile preclinical models of human T cell responses. *J Immunol* **191**, 583-593, doi:10.4049/jimmunol.1300483 (2013).

Declarations

Acknowledgements:

General: Authors wish to thank Ms. Linda Jones for technical support. We also wish express thanks to QIMR Berghofer animal facility staff.

Funding: We acknowledge support from Atara Biotherapeutics and Elicio Therapeutics.

Author Contributions: V.D., L.K.M., M.P.S., P.C.D. and R.K. designed the study and contributed to the drafting of the manuscript. V.D., and K.B., conducted mice immunogenicity studies. V.D., A.J., L.M.S., J.Z., L.K.M., M.P.S., and P.C.D. contributed to data analysis. V.D., A.J., L.M.S., G.A., M.S., and J.Z. conducted experimental studies. C.M.H. reviewed the manuscript. R.K. and P.C.D. provided supervision and oversaw final manuscript preparation. All authors reviewed and approved the version for publication.

Competing Interests: L.K.M., M.P.S., A.J., L.M.S., J.Z., C.M.H., and P.C.D. are employees of Elicio Therapeutics and as such receive salary and benefits, including ownership of stock and stock options from the company. V.D. and R.K. hold international patents on EBV vaccine and immunotherapy; R.K. acts as consultant for Atara Biotherapeutics. R.K. is on the Scientific Advisory Board of Atara Biotherapeutics. The authors declare no other competing interests. The authors have no other relevant affiliations or financial involvement with any organization or entity with a financial interest in, or financial conflict with the subject matter or materials discussed in the manuscript, apart from those disclosed.

Figures

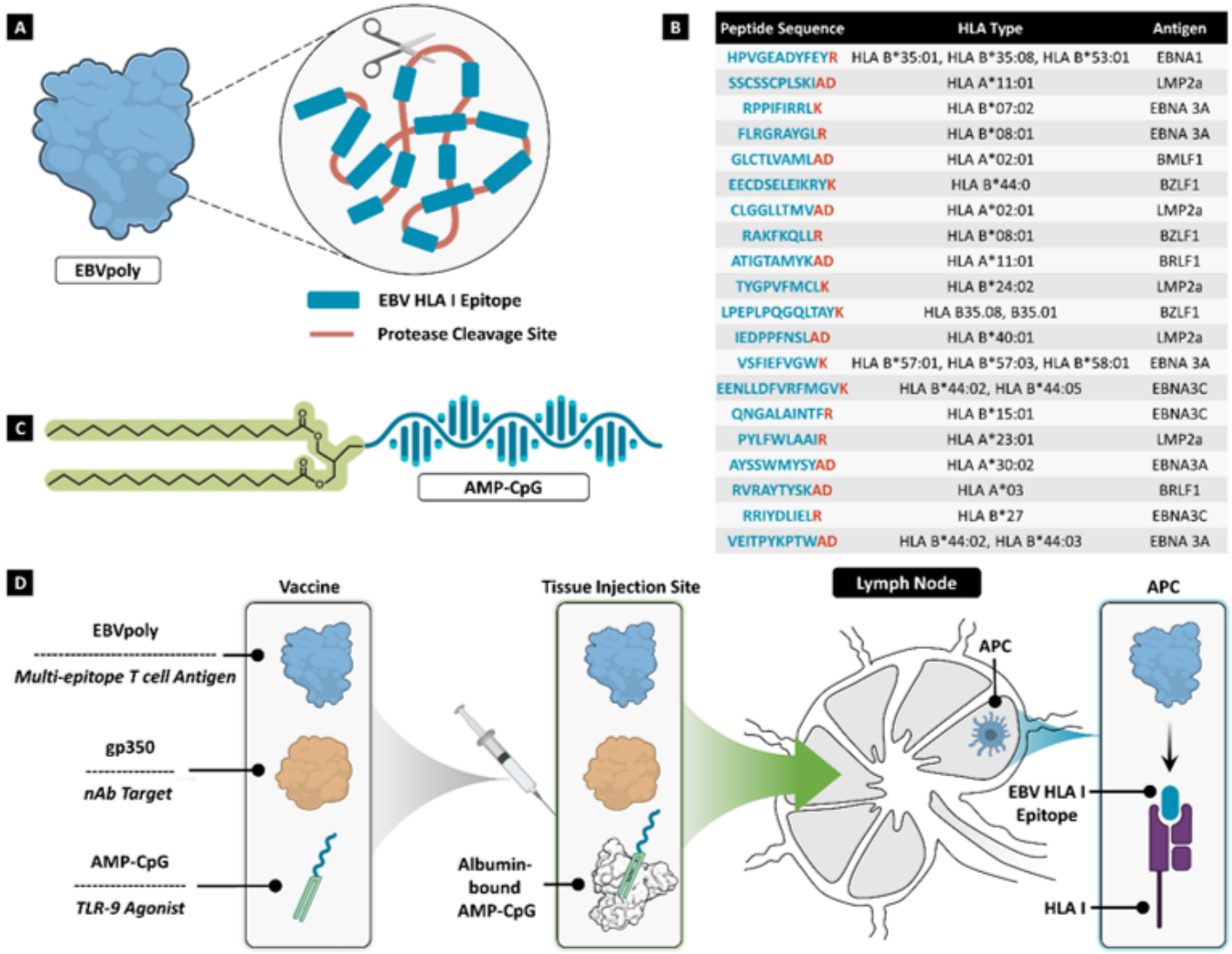

Peptide Sequence	HLA Type	Antigen
HPVGEADYFEYR	HLA B*35:01, HLA B*35:08, HLA B*53:01	EBNA1
SSCSSCPLSKIAD	HLA A*11:01	LMP2a
RPPIFIRRLK	HLA B*07:02	EBNA 3A
FLRGRAYGLR	HLA B*08:01	EBNA 3A
GLCTLVAMLAD	HLA A*02:01	BMLF1
EECDSELEIKRYK	HLA B*44:0	BZLF1
CLGGLLTMVAD	HLA A*02:01	LMP2a
RAKFKQLLR	HLA B*08:01	BZLF1
ATIGTAMYKAD	HLA A*11:01	BRLF1
TYGPVFMCLK	HLA B*24:02	LMP2a
LPEPLPQGQLTAYK	HLA B35.08, B35.01	BZLF1
IEDPPFNSLAD	HLA B*40:01	LMP2a
VSFIEFVGWK	HLA B*57:01, HLA B*57:03, HLA B*58:01	EBNA 3A
EENLLDFVRFMGVK	HLA B*44:02, HLA B*44:05	EBNA3C
QNGALAINTFR	HLA B*15:01	EBNA3C
PYLFWLAAIR	HLA A*23:01	LMP2a
AYSSWMYSYAD	HLA A*30:02	EBNA3A
RVRAYTYSKAD	HLA A*03	BRLF1
RRIYDLIELR	HLA B*27	EBNA3C
VEITPYKPTWAD	HLA B*44:02, HLA B*44:03	EBNA 3A

Figure 1

Design of a lymph node-targeted subunit vaccine for EBV.

(A) Schematic representation of EBVpoly protein, showing the “beads on a string” structure. EBVpoly is a polyprotein containing 20 $CD8^+$ T cell epitopes from eight EBV antigens. The peptide sequence, HLA type and source antigen for each of the epitopes is listed in **(B)**, with the proteasome liberation sequence highlighted in red. **(C)** Schematic representation of the adjuvant, AMP-CpG. **(D)** Vaccine design and mechanism of vaccination including delivery to the lymph nodes following subcutaneous injection. EBVpoly is an engineered multi-epitope protein immunogen consisting of multiple HLA-restricted T cell target epitopes; gp350 is a predominant viral target for neutralizing antibody responses; AMP-CpG is a lymph node targeted TLR-9 agonist. AMP-CpG binds to endogenous albumin at the injection site and albumin chaperones AMP-CpG into the lymph nodes in concert with passive transport of EBVpoly and gp350. Lymph node APCs internalize and process EBVpoly and the individual epitopes are presented on HLA Class I to $CD8^+$ T cells.

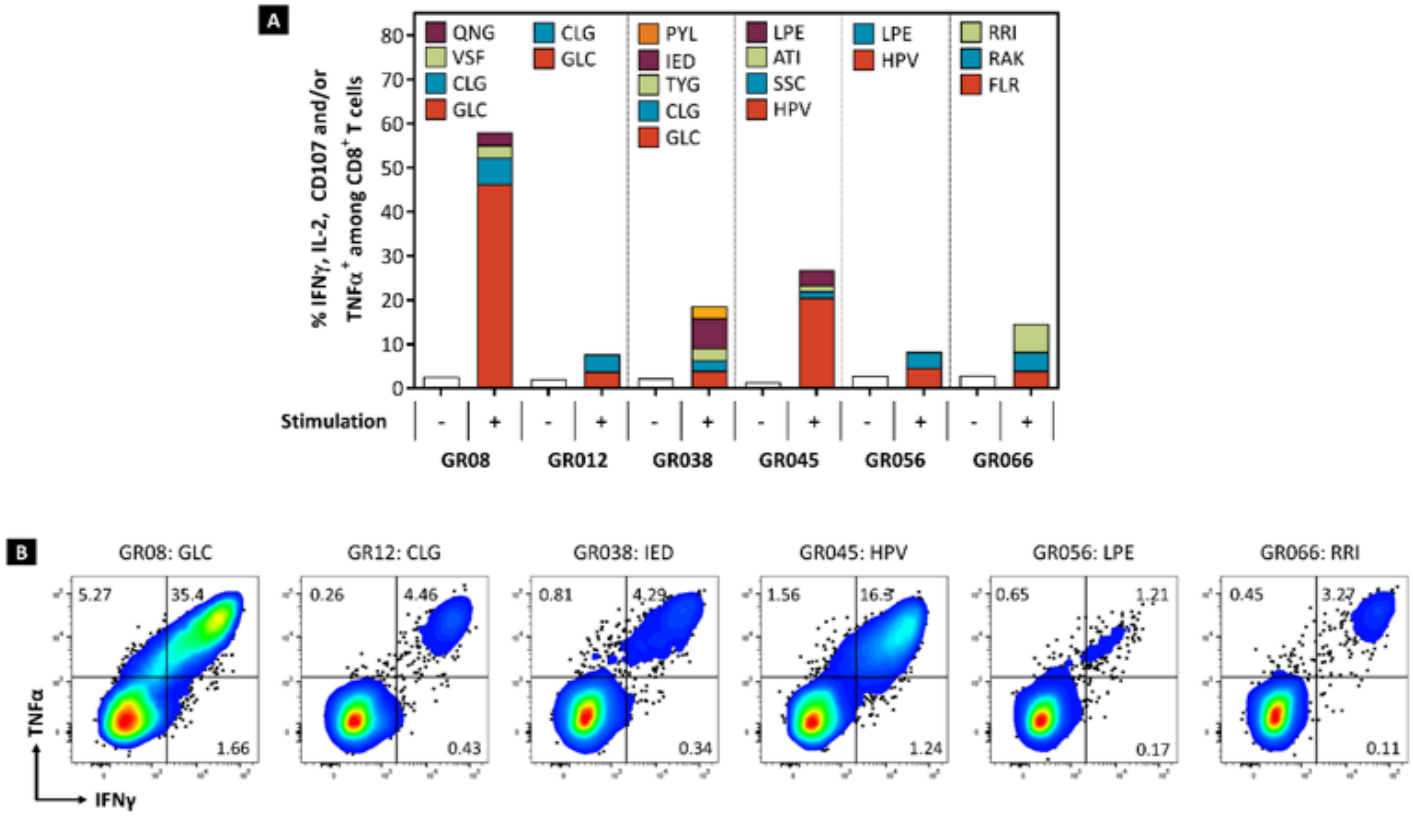

Figure 2

EBVpoly stimulation of human PBMCs expands EBV-specific CD8$^+$ T cells.

(A) PBMCs from healthy EBV seropositive patients were stimulated with EBVpoly for 1 hour, then expanded for 14 days in the presence of IL-2. Expanded PBMCS were re-stimulated with the individual antigen peptides from EBVpoly in an ICS assay. Shown are frequencies of IFNg, IL-2, TNFα and/or CD107$^+$ CD8$^+$ T cells. White bars indicate no peptide stimulation. Colored bars represent responses to each annotated peptide designated based on the first three amino acid residues of the cognate epitope. **(B)** Shown are representative flow cytometry dot plots of IFNg vs TNFα for each donor demonstrating responses to the designated peptide re-stimulation.

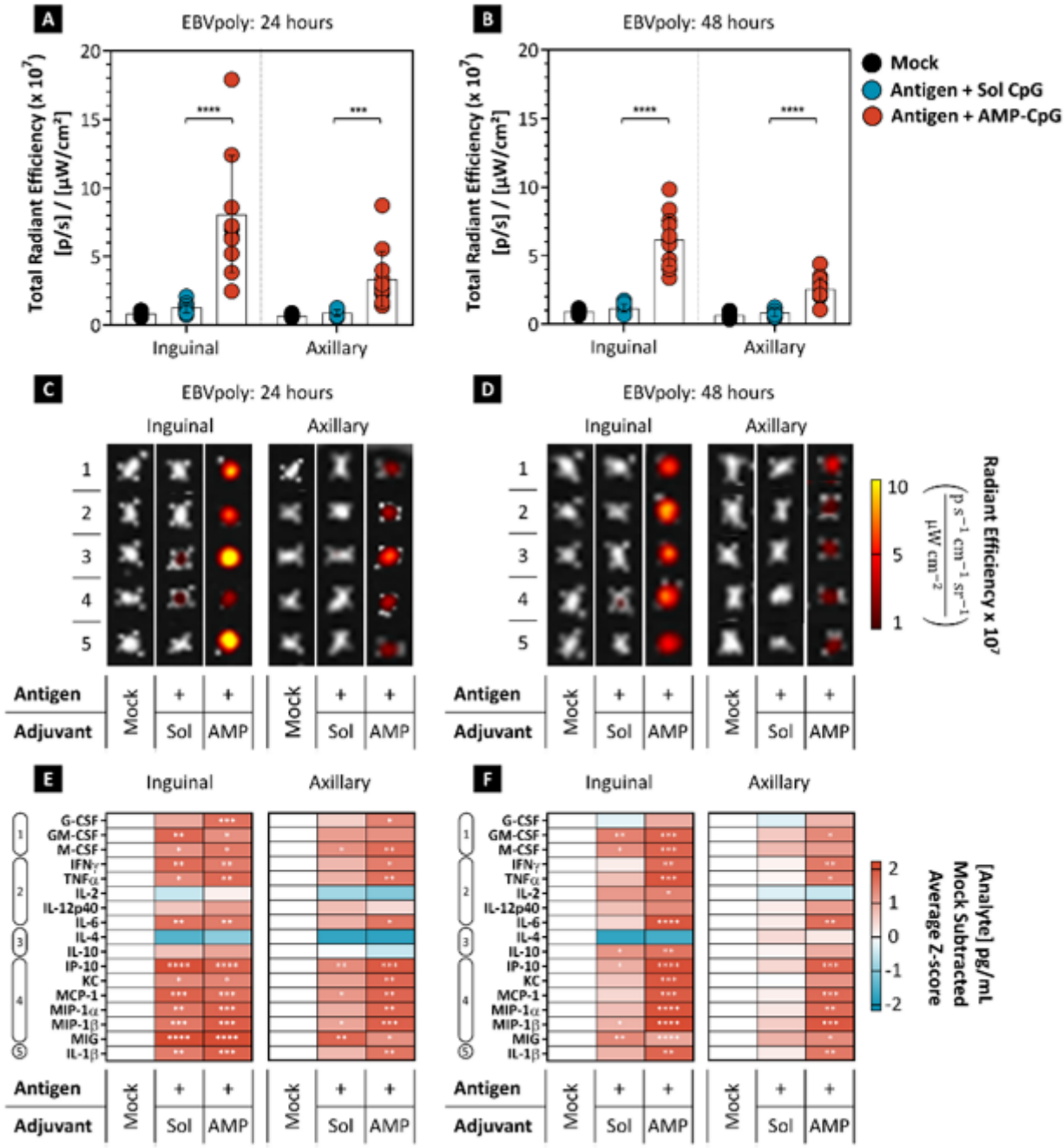

Figure 3

AMP-CpG enhances delivery of EBVpoly to the lymph node alongside comprehensive immune activation.

C57Bl/6J mice were immunized with 8 µg EBVpoly-AF594 and 10 µg gp350-AF647 admixed with 1.2 nmol soluble- or AMP-CpG. **(A-D)** Quantification of total radiant efficiency in inguinal and axillary lymph nodes analyzed *ex vivo* by IVIS at **(A)** 24 and **(B)** 48 hours post primer dose. Mock treatments represent fluorescence-negative controls collected from mice receiving equivalent amounts of AMP-CpG and unlabeled antigens. **(C, D)** IVIS images of five representative lymph nodes in **A** and **B**. **(E, F)** Quantification of cytokine concentrations in lymph nodes from **A** and **B** by Luminex. Depicted are mock-subtracted

average Z-scores of protein analyte concentrations in lymph nodes. Cytokines are clustered into functional groups: (1) growth factors, (2) Th1/inflammatory cytokines, (3) Th2/regulatory cytokines, (4) chemokines, and (5) inflammasome associated cytokines. Mock-treated animals were administered vehicle alone. Values depicted are mean ± standard deviation. *$p < 0.05$; **$p < 0.001$; ***$p < 0.0005$; ****$p < 0.0001$.*

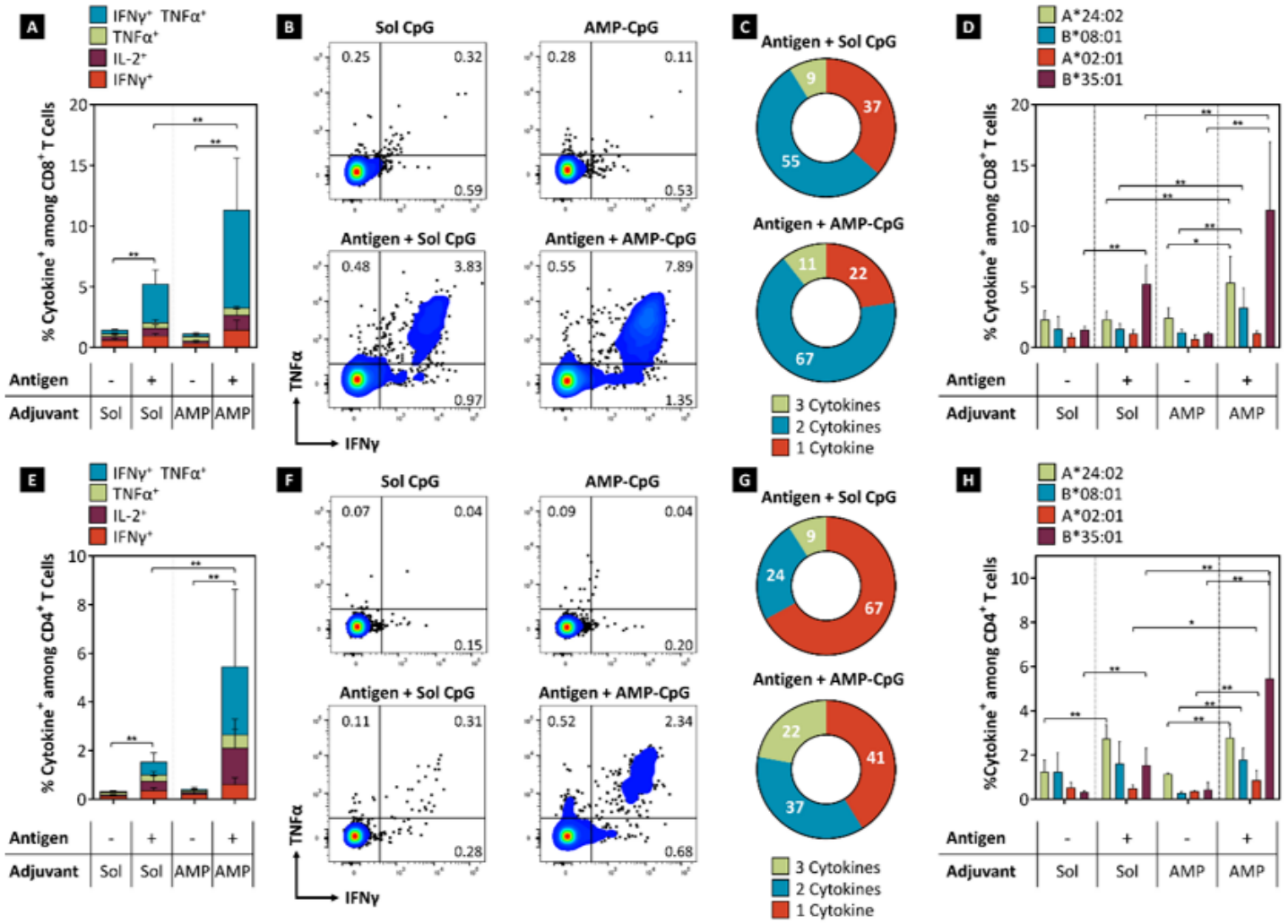

Figure 4

Vaccination with AMP-CpG induces robust polyfunctional EBV-specific T cell responses in splenocytes.

(A-H) HLA-B*35:01 transgenic mice (n = 6 per vaccine group and n = 4 per control group) were immunized on Weeks 0, 3 and 6 with 40 µg EBVpoly and 10 µg gp350 proteins admixed with 1.2 nmol soluble- or AMP-CpG and T cell responses were analyzed on Week 7. Control groups were immunized with soluble-CpG or AMP-CpG alone. Splenocytes were stimulated with **(A-D)** EBV $CD8^+$ T cell peptides or **(E-H)** gp350 OLPs in an ICS assay. **(A, E)** Shown are frequencies of IFNg, IL-2, TNFα and IFNg TNFα double positive

CD8$^+$ or CD4$^+$ T cells, with **(B, F)** corresponding representative dot plots. **(C, G)** Pie chart representations of the functional T cell profiles. Pies represent the capacity of T cells to secrete any (1, 2 or 3) of the three cytokines IFNg, TNFα and IL-2. **(D, H)** Frequencies of cytokine$^+$ **(D)** CD8$^+$ T cells and **(H)** CD4$^+$ T cells in splenocytes to indicated HLA transgenic mice. Values depicted are mean ± standard deviation. * *p < 0.05; ** p < 0.01 by two-sided Mann-Whitney test applied to cytokine+ T cell frequencies. If statistics are not indicated, then the comparison was not significant.*

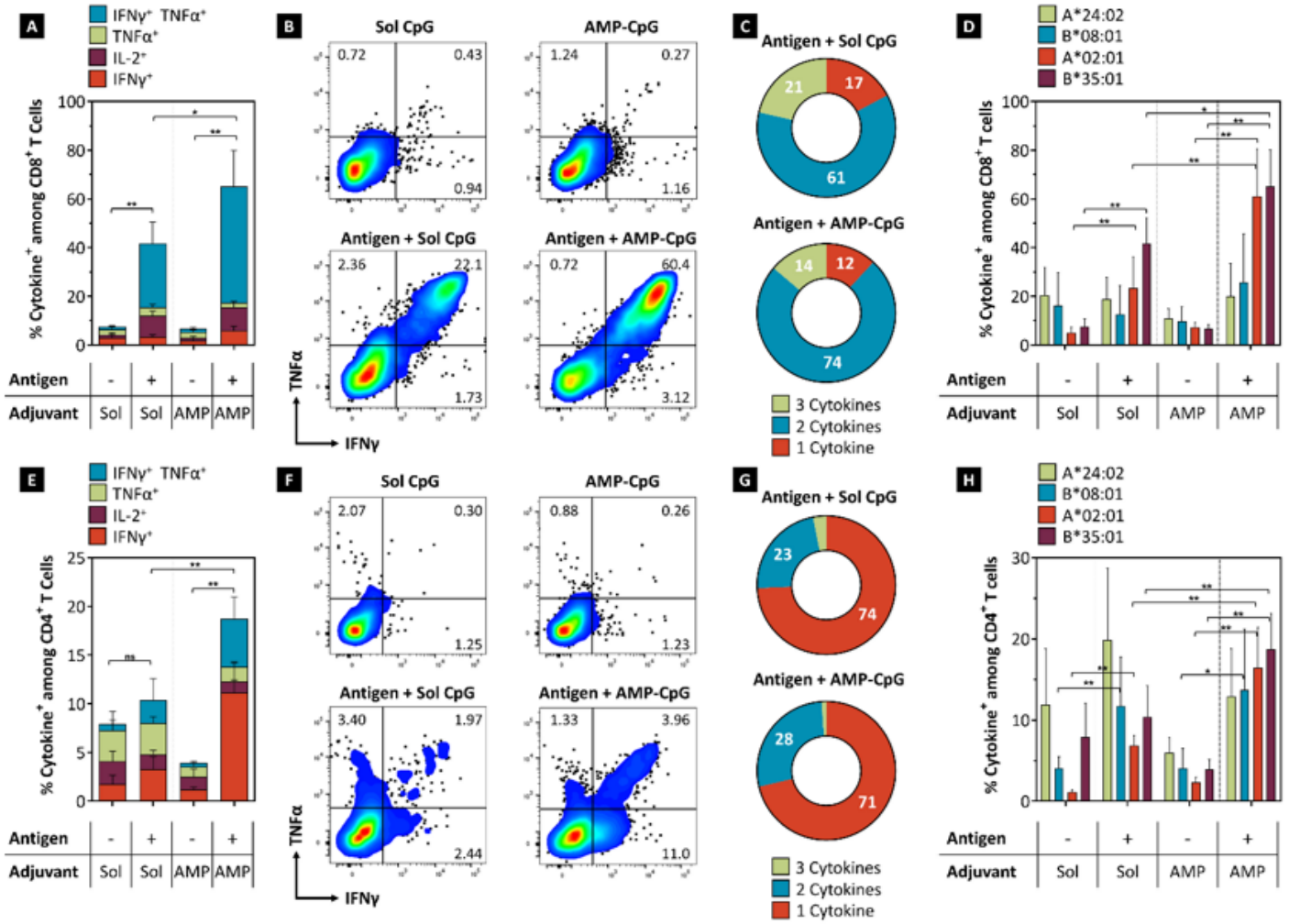

Figure 5

Vaccination with AMP-CpG induces robust polyfunctional EBV-specific T cell responses in expanded splenocytes.

(A-H) HLA-B*35:01 transgenic mice (n = 6 per vaccine group and n = 4 per control group) were immunized on Weeks 0, 3 and 6 with 40 µg EBVpoly and 10 µg gp350 proteins admixed with 1.2 nmol soluble- or AMP-CpG and T cell responses were analyzed on Week 7. Control groups were immunized with soluble-CpG or AMP-CpG alone. Splenocytes were collected on Week 7 and stimulated with IL-2 and **(A-D)** EBV

CD8$^+$ T cell peptides or **(E-H)** gp350 OLPs for 10 days. Expanded splenoctyes were restimulated with **(A-D)** CD8$^+$ T cell peptides and **(B-H)** gp350 OLPs in an ICS assay. **(A, E)** Shown are frequencies of IFNg, IL-2, TNFα and IFNg TNFα double positive CD8$^+$ or CD4$^+$ T cells, with **(B, F)** corresponding representative dot plots. **(C, G)** Pie chart representations of the functional T cell profiles. Pies represent the capacity of T cells to secrete any (1, 2 or 3) of the three cytokines IFNg, TNFα and IL-2. **(D, H)** Frequencies of cytokine$^+$ **(D)** CD8$^+$ T cells and **(H)** CD4$^+$ T cells in splenocytes to indicated HLA transgenic mice. Values depicted are mean ± standard deviation. * *p < 0.05; ** p < 0.01 by two-sided Mann-Whitney test applied to cytokine+ T cell frequencies. If statistics are not indicated, then the comparison was not significant.*

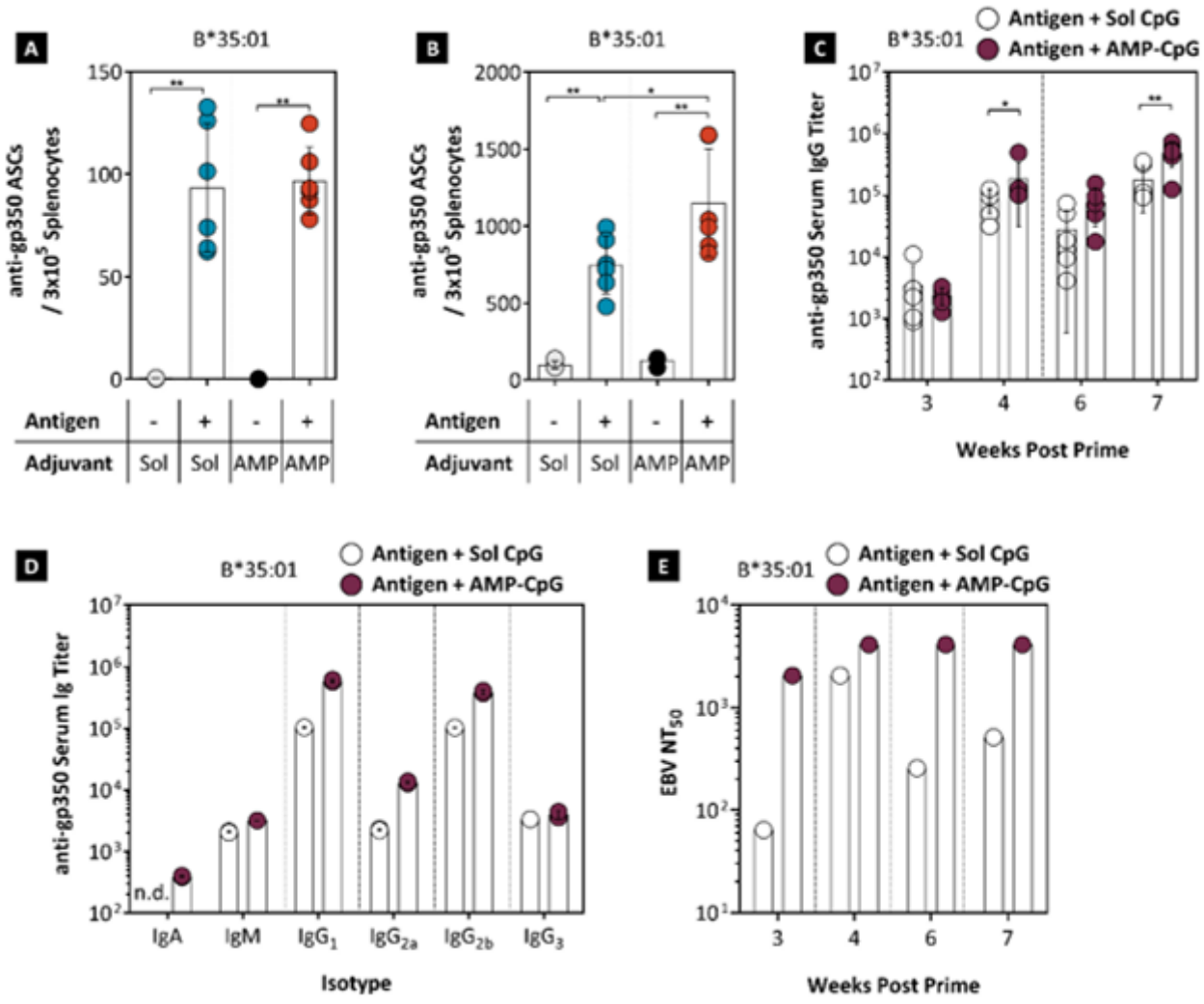

Figure 6

AMP-CpG induces strong serum IgG and neutralizing antibody responses targeting gp350.

HLA-B*35:01 transgenic mice (n = 6 per vaccine group and n = 4 per control group) were immunized on Weeks 0, 3 and 6 with 40 µg EBVpoly and 10 µg gp350 proteins admixed with 1.2 nmol soluble- or AMP-

CpG. Control groups were immunized with soluble-CpG or AMP-CpG alone. Humoral responses to gp350 were assessed in splenocytes and serum from immunized mice on Week 7 by antibody secreting cells (ASC) ELISPOT, ELISA or neutralization assay. Shown are **(A)** *ex vivo* ASC ELISPOT measured frequency of gp350-specific ASCs per $3x10^5$ splenocytes, **(B)** expanded ASC ELISPOT measured frequency of gp350-specific ASCs per $3x10^5$ splenocytes, **(C)** longitudinal serum IgG titers, **(D)** Ig subtype titers at Week 7 in pooled serum samples and **(E)** longitudinal EBV neutralization titers in pooled serum samples. Values depicted are mean ± standard deviation. Not detected (n.d.) values are shown on the baseline. ** p < 0.05; ** p < 0.01 by two-sided Mann-Whitney test. If statistics are not indicated, then the comparison was not significant.*

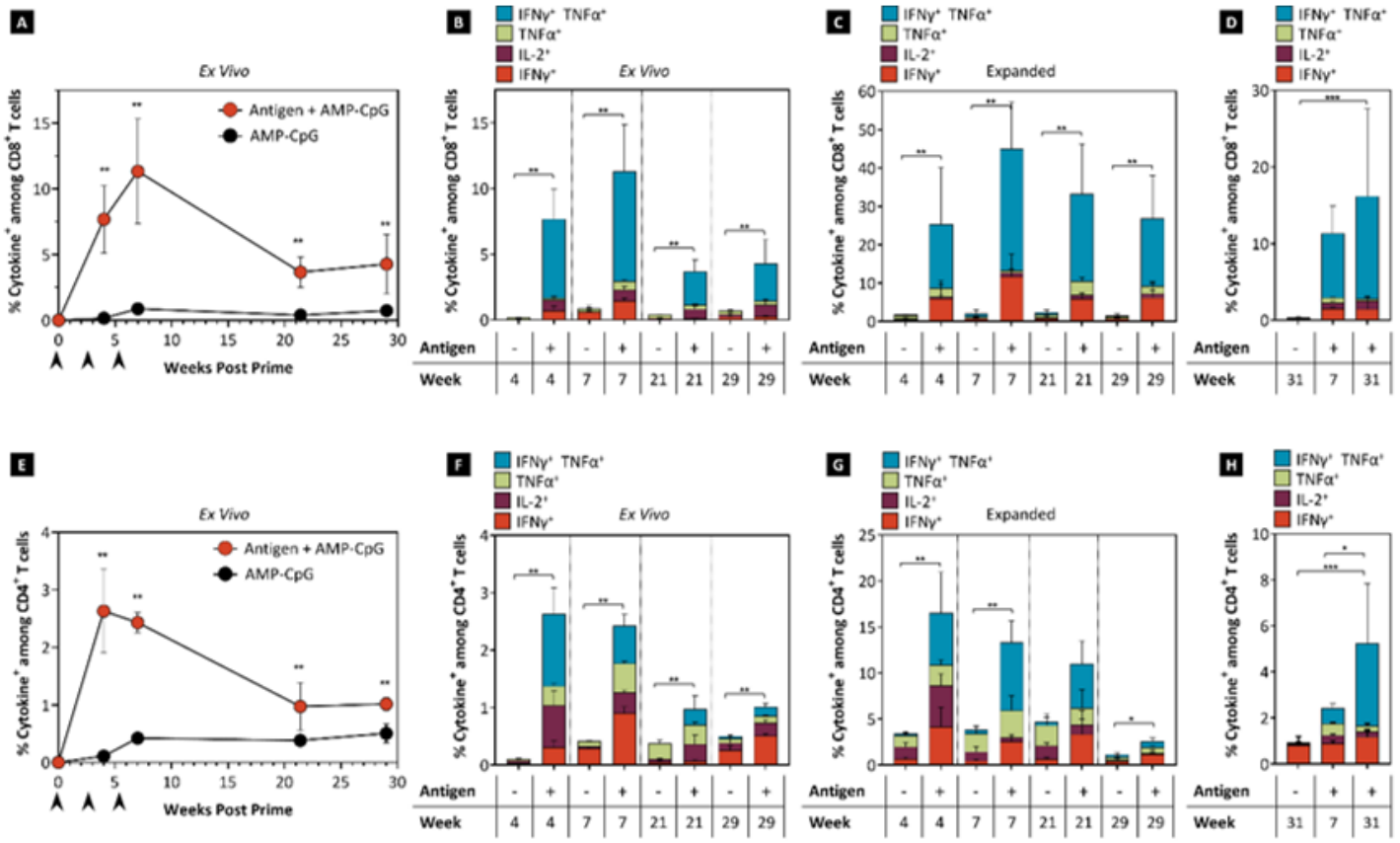

Figure 7

Vaccination with AMP-CpG maintains EBV-specific $CD8^+$ and $CD4^+$ T cells responses for >7 months.

(A-H) HLA-B*35:01 transgenic mice (n = 9 per vaccine group and n = 5 per control group) were immunized on Weeks 0, 3 and 6 with 40 µg EBVpoly and 10 µg gp350 proteins admixed with 1.2 nmol AMP-CpG and T cell responses were analyzed at long term timepoints. The control group was immunized with AMP-CpG alone. Splenocytes were stimulated with **(A-D)** EBV $CD8^+$ T cell peptides or **(E-H)** gp350 OLPs in an ICS

assay. Shown are frequencies of total IFNg, IL-2, and TNFα **(A)** $CD8^+$ or **(E)** $CD4^+$ T cells over time; polyfunctional cytokine$^+$ **(B)** $CD8^+$ or **(F)** $CD4^+$ T cell frequencies at different timepoints; *in vitro* stimulated cytokine+ **(C)** $CD8^+$ or **(G)** $CD4^+$ T cell frequencies at different timepoints; and Week 31 **(D)** $CD8^+$ or **(H)** $CD4^+$ T cell response to a recall vaccination at Week 30, compared to Week 7 peak responses. Values depicted are mean ± standard deviation. Black arrows indicate immunization days. * *$p < 0.05$; ** $p < 0.01$ by two-sided Mann-Whitney test applied to cytokine+ T cell frequencies. If statistics are not indicated, then the comparison was not significant.*

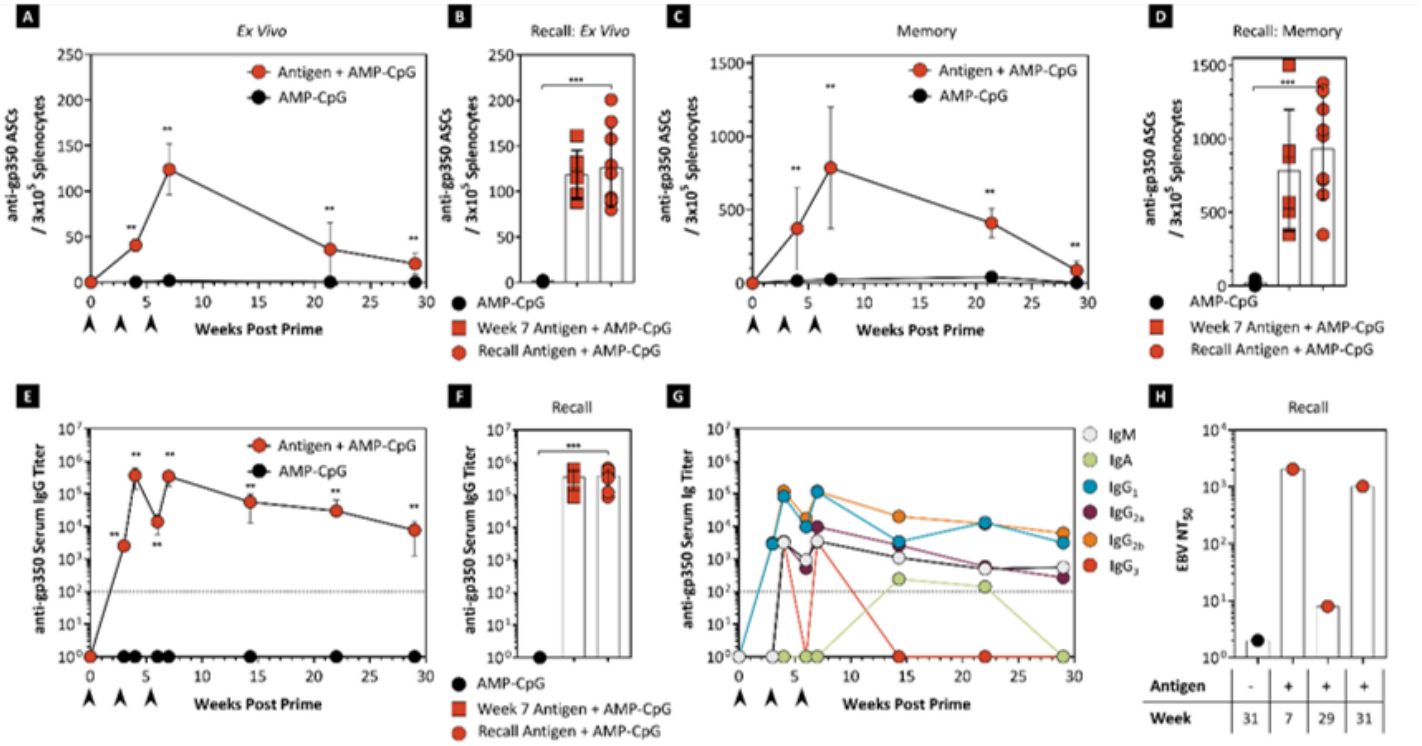

Figure 8

Vaccination with AMP-CpG induces durable gp350-specific IgG responses.

HLA-B*35:01 transgenic mice (n = 9 per vaccine group and n = 5 per control group) were immunized on Weeks 0, 3 and 6 with 40 ug EBVpoly and 10 ug gp350 proteins admixed with 1.2 nmol AMP-CpG. The control group was immunized with AMP-CpG alone. Humoral responses to gp350 were assessed in splenocytes and serum from immunized mice at Week 7 by antibody secreting cells (ASC) ELISPOT or ELISA assay. Shown are **(A)** *ex vivo* ASC ELISPOT measured frequency of gp350-specific ASCs per $3x10^5$ splenocytes, **(B)** Week 31 *ex vivo* ASC recall response to a recall vaccination at Week 30, **(C)** expanded memory ASC ELISPOT measured frequency of gp350-specific ASCs per $3x10^5$ splenocytes, **(D)** Week 31 memory ASC recall response to a recall vaccination at Week 30, **(E)** longitudinal serum IgG titers, **(F)** Week 31 IgG titers to a recall vaccination at Week 30, **(G)** longitudinal Ig subtype titers in pooled serum

samples, and **(H)** Week 31 recall EBV neutralization titers to a recall vaccination at Week 30, compared to Week 7 peak responses using pooled serum samples. Values depicted are mean ± standard deviation. Black arrows indicate immunization days. ** p < 0.05; ** p < 0.01; *** P < 0.001 by two-sided Mann-Whitney test.*

Supplementary Files

This is a list of supplementary files associated with this preprint. Click to download.

- Supplement.docx